NUMERICAL SIMULATIONS FOR THE BEAM-INDUCED ELECTRON CLOUD IN IN THE LHC BEAM SCREEN

O. Brüning, CERN, Geneva, Switzerland

Abstract

The following work summarises simulation results obtained at CERN for the beam-induced electron cloud and looks at possible cures for the heat load in the LHC beam screen. The synchrotron radiation in the LHC creates a continuous flow of photoelectrons. These electrons are accelerated by the electric field of the bunch and hit the vacuum chamber on the opposite side of the beam pipe where they create secondary electrons which are again accelerated by the next bunch. For a large secondary emission yield the above mechanism leads to an exponential growth of the electron cloud which is limited by space charge forces. The simulations use a two-dimensional mesh for the space charge calculations and include the effect of image charges on the vacuum chamber wall. Depending on the quantum yield for the production of photoelectrons, the secondary emission yield and the reflectivity, the heat load can vary from 0.1 W/m to more than 15 W/m.

1 INTRODUCTION

The energy deposition due to the electron cloud on the vacuum chamber walls can give an important contribution to the total heat load on the LHC liner. The current budget of the LHC cryogenic system is based on an electron cloud induced heat load of $P \approx 0.2$ W/m and cannot tolerate a heat load of more than $P = 0.5$ W/m. Thus, the design of the beam screen must assure a heat load which is smaller than this amount. However, numerical simulations of the electron dynamics inside the vacuum chamber showed that the heat load can reach values as large as $P = 15$ W/m or more. Currently there are two different programs which are used for estimating the heat load in the LHC beam screen due to photoelectrons: one code from M. Furman which was developed at LBL [1] and one based on a program by F. Zimmermann [2] which was further developed at CERN in order to study the heat load in the beam screen [3]. The availability of two independent simulation programs for the heat load generation in the beam screen has proven to be extremely useful. A continuous comparison of the results generated by the two programs indicated several weak points in the algorithms and finally led to an improvement of both programs. While the results initially disagreed by more then a factor of two, they now differ by less then 20%, giving us good confidence in the results.

The following work summarises the simulation results obtained at CERN and looks at possible cures for the heat load in the beam screen. The work is part of a crash program at CERN which aims to identify the key parameters which determine the net heat load in the liner and to measure the relevant parameters of the vacuum chamber [4].

2 SIMULATION MODEL

We assume a Gaussian longitudinal bunch distribution and cut the bunch into 50 slices. During the bunch passages we generate new photoelectrons. For protons at 7 TeV the total number of photoelectrons with energies larger than 4 eV (the work function of Cu) is approximately $N_{bunch} \cdot Y \cdot 0.17$ photons per bunch, where N_{bunch} is the number of protons per bunch and Y the photoelectron yield [3]. For all calculations we assumed a Gaussian energy distribution of the photoelectrons around 7 eV and a width of $\sigma_{pe} = 5\,eV$.

The electrons are modelled by macro-particles. We generate a total of 1000 macro particles per bunch and the number of macro-particles generated per beam slice is proportional to the number of protons inside the slice. For each slice we first generate the new photoelectrons and then evaluate the force of the beam slice (including the beam image charges on the vacuum chamber wall) on the electrons.

The gap between two bunches is again divided into 50 steps, allowing a proper modelling of the particle motion under the influence of space charge and detecting the electron losses at the proper positions. In all cases we calculate the space charge on a two dimensional 25×25 mesh and include the contributions from image charges on the vacuum chamber wall (the calculation of the image charges is based on an elliptical boundary).

Once an electron reaches the boundary of the vacuum chamber the program calculates the secondary emission yield of the incident electron as a function of its energy and incident angle with respect to the surface normal. The charge of the emitted macro particle is given by the product of the initial charge and the secondary emission yield $\delta\,(E,\theta)$. For the secondary emission yield we assume [5]

$$\delta\,(E,\theta) = \delta_{max} \cdot 1.11 \cdot \left(\frac{E}{E_{max}}\right)^{-0.35} \times \quad (1)$$

$$\left(1 - \exp\left[-2.3 \cdot \left(\frac{E}{E_{max}}\right)^{1.35}\right]\right)/max\,(\cos\theta, 0.2)\,,$$

where θ is the angle of the incident electron with respect to the surface normal, E the electron energy, E_{max} the energy for which the secondary emission yield has a maximum and δ_{max} the maximum secondary emission yield for normal incidence of the electron. In the following we assume $E_{max} = 300\ eV$ for all simulations and limit the value of $\cos\theta$ to values larger then 0.2.

The energy distribution of the secondary electrons is modelled by a half Gaussian centered at 0 eV and with an rms width between $\sigma_{se} = 3\ eV$ and $\sigma_{se} = 20\ eV$. The value of σ_{se} determines how many secondary electrons remain inside the vacuum chamber before the next bunch arrives.

All results presented here are based on the nominal LHC beam parameters [6].

3 SECONDARY EMISSION YIELD

In this section we look for the maximum secondary yield coefficient δ_{max} for which we do not observe an exponential growth of the electron cloud. If the secondary emission coefficient of the vacuum chamber is much smaller than this critical value (SEY_{crit}), the heat loss will be approximately proportional to the number of synchrotron light photons and the photon yield. If it is larger than SEY_{crit}, the heat loss will be determined by the value of δ_{max} and even a single electron, e.g. from residual gas ionisation, is sufficient to trigger the build up of an electron cloud. Clearly, when designing a beam screen for the LHC vacuum chamber it is necessary to achieve a secondary emission coefficient which is smaller than SEY_{crit} and it becomes important to understand how SEY_{crit} depends on the beam parameters and the vacuum chamber geometry. In order to determine SEY_{crit}, we neglect the space charge effects and generate photoelectrons only for the first bunch. Looking at the evolution of the number of electrons per unit length over 60 bunch passages, the electron density will decrease if the secondary emission yield is smaller then the critical value. If the secondary emission yield is larger, the electron density will grow exponentially. Table 1 shows the SEY_{crit} for two different values of σ_{se}. In all cases, SEY_{crit} is smaller than the secondary emission yield of copper ($\delta_{max} \approx 2.0$), the proposed surface material for the LHC liner. The larger the value of σ_{se} the more secondary

Field	No Field		Dipole		Quadrupole	
σ_{se} [eV]	3.0	10.0	3.0	10.0	3.0	10.0
SEY_{crit}	1.4	1.7	1.2	1.4	13	14

Table 1: *Critical secondary emission yield (SEY_{crit}) for different magnetic field configurations and energy distributions for the secondary electrons (σ_{se}).*

electrons reach the opposite side of the vacuum chamber before the next bunch arrives. Because these are all low energetic electrons ($E \ll E_{max}$) they are absorbed by the vacuum chamber without generating new secondary electrons and the critical secondary emission yield SEY_{crit} increases with increasing σ_{se}. For the cases with magnetic field, the particles move effectively only along the field lines and only the velocity component parallel to the field lines determines the transit time of the electrons from one side of the vacuum chamber to the other. This reduces the number of electrons which are lost before the next bunch arrives and SEY_{crit} is smaller for the cases with magnetic field than in the case without field lines.

The above results suggest a particularly high heat load for small values of σ_{se}. However, electrons with small energies are also more strongly affected by their own space charge field. Depending on the secondary emission yield, one finds that for the LHC parameters that space charge
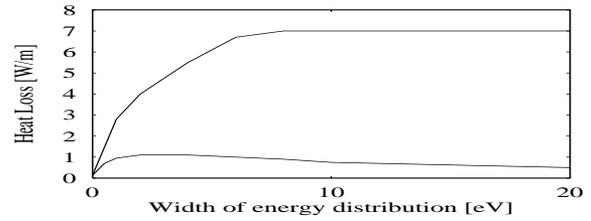

Figure 1: *Heat load versus the width of the initial energy distribution of the secondary electrons for $Y = 0.2$ and $B = 8.4$ T. Top: $\delta_{max} = 1.8$. Bottom: $\delta_{max} = 1.066$.*

fields are relevant for electron energies less than 1 eV or 10 eV [3] depending on whether the secondary emission yield is larger or smaller than SEY_{crit}. Fig.1 illustrates this effect with simulation data for two different values of the secondary emission yield and the case of an 8.4 T dipole field.

	No Field		Dipole		Quadrupole	
δ_{max}	1.3	1.8	1.3	1.8	1.3	1.8
P [W/m]	2.4	6.2	1.5	5.2	0.06	0.06

Table 2: *Heat loss for different magnetic field configurations and secondary emission yields for a uniform distribution of photoelectrons along the azimuthal direction of the vacuum chamber (R = 1.0): Y = 0.1, σ_{se} = 5 eV.*

4 HIGH REFLECTIVITY

In case of high reflectivity the photoelectrons are approximately uniformly distributed over the surface of the beam screen. Table 2 gives the corresponding heat load in the liner for three magnetic field configurations and two different secondary emission yields (the secondary emission yields are taken from [7]). In all cases we assumed nominal LHC beam parameters and a photon yield of $Y = 0.1$. The largest heat deposition occurs in the field free region and the lowest in the quadrupole field. In the case of strong magnetic field lines, the electrons are effectively accelerated only along the field lines. Hence, they experience only a fraction of the full kick when a bunch passes by. Because the heat loss in the liner is proportional to the average energy of the electrons the heat loss decreases with decreasing kick strength. The net kick in the quadrupole field is smaller than the kick in the dipole field or the field free region.

5 LOW REFLECTIVITY

For small reflectivity, the photoelectrons are mainly generated within the horizontal plane of the beam screen. Thus, in the presence of strong vertical magnetic field lines the electrons experience only a small effective kick when a bunch passes by and the heat loss is smaller than in the case of high reflectivity. Table 3 illustrates this effect for three different magnetic field configurations and three different

secondary emission yields. In all cases we assumed the nominal beam parameters and a photon yield of $Y = 0.1$. In order to account for a small reflectivity, we generate 90% of the synchrotron light photons with a Gaussian angular distribution with $\sigma_\phi = 22.5^o$ at one side of the vacuum chamber. 10% of the photoelectrons are still uniformly distributed in the transverse plane (R = 0.1). The heat loss inside the dipole magnets decreases from 1.5 W/m to 0.15 W/m for $\delta_{max} = 1.2$. However, in case the secondary emission yield is larger than SEY_{crit} the heat loss is determined by δ_{max} and the fact that 10% of the photoelectrons are still uniformly distributed along the azimuthal direction leads to the same heat load as in the case of high reflectivity. For example, for $\delta_{max} = 1.3$ which is just slightly larger than $SEY_{crit}(\sigma_{se} = 5 \text{ eV})$ the heat loss takes the same value as for the case with high surface reflectivity.

Field	No Field		Dipole			Quadrupole	
δ_{max}	1.3	1.8	1.2	1.3	1.8	1.3	1.8
P [W/m]	2.4	6.2	0.15	1.5	5.0	0.02	0.02

Table 3: *Heat loss for different magnetic field configurations and secondary emission yields: Y = 0.1, σ_{se} = 5 eV. 90% of the synchrotron light photons are generated at one side of the vacuum chamber. 10% of the photoelectrons are uniformly distributed in the azimuthal direction.*

6 EXTERNAL FIELDS

It has been proposed to reduce the electron build up in regions without magnetic field lines by an external solenoid field of 50 Gauss. The solenoid field bends the electron trajectory back into the vacuum chamber and the photoelectrons are re-absorbed before they are accelerated by the next passing bunch. However, this solution only works in the field free regions of the LHC. In the presence of strong vertical magnetic field lines the electrons can essentially move only parallel to the field lines and one can reduce the heat load inside the dipole magnets only by generating a force parallel to the field lines. For example, stretched wires in the four corners of the liner with a potential of 20 Volts between the wires and the liner wall decreases the heat loss in the beam screen from $5.2\ W/m$ to less than $0.2\ W/m$ [3]. However, it is not clear if such a solution could be realised from the hardware and aperture point of view. Nevertheless, it illustrates how the low energetic secondary electrons are influenced even by very small external perturbations.

7 SUMMARY

Assuming a uniform distribution of the photoelectrons in the azimuthal direction and a secondary emission yield $\delta_{max} > SEY_{crit}$ the numerical simulations indicate heat losses which are more than an order of magnitude higher than the tolerable limit given by the cryogenic system ($P_{CS} < 0.2$ W/m). Only the heat losses inside the quadrupoles are smaller than P_{CS}.

Generating the photoelectrons mainly in the horizontal plane of the beam screen (low surface reflectivity) reduces the heat losses in regions with strong magnetic field lines. Assuming, for example, a Gaussian angular distribution of the photoelectrons with $\sigma_\phi = 22.5^o$ at one side of the vacuum chamber reduces the heat losses in the dipole magnets from 5.2 W/m to 0.2 W/m. However, this method is only efficient if the secondary emission yield is smaller than SEY_{crit}. For $\delta_{max} > SEY_{crit}$ the heat loss is determined by δ_{max} and even a small fraction of the photoelectrons which are generated above or below the passing beam lead to a heat loss larger than P_{CS}.

For the LHC, this indicates two steps for reducing the heat loss inside the dipole magnets. First, the secondary emission coefficient of the surface material must be smaller than SEY_{crit}. This can be done by coating the inner surface of the liner with TiN or TiZr. Second, the reflectivity of the liner should be as small as possible where the synchrotron light hits the liner. One possibility is to construct a ribbed vacuum chamber where the synchrotron light hits the surface of the liner parallel to the surface normal. Both strategies are analysed at CERN. Alternatively, one can generate an electrostatic potential across the vacuum chamber. However, it is not clear if such a solution is feasible from the hardware and aperture point of view.

Inside the field free region, where the heat losses are the largest, the surface reflectivity has no influence on the heat losses due to the electron cloud. Here, the electron cloud density must be reduced by external fields. For example, one can utilise a weak solenoid field (50 Gauss) for this purpose.

In all cases analysed, the heat loss inside the quadrupole magnets is smaller than the limit imposed by the cryogenic system.

8 REFERENCES

[1] M. A. Furman, "Comments on the Electron Cloud Effect in the LHC Dipole e=Bending Magnets," KEK Proceedings 97-17,p234, December 1997 (Proc. MBI-97 workshop, KEK, Tsukuba, Japan, 15-18 July; Y.H. Chin, ed.).

[2] F. Zimmermann "A Simulation Study of Electron-Cloud instability and Beam-Induced Multipactoring in the LHC" LHC Project Report 95 (1997).

[3] O. Brüning, "Simulations for the Beam-Induced Electron Cloud in the LHC beam screen with Magnetic Field and Image Charges" LHC Project Report 158 (1997).

[4] V. Baglin et al, "Beam-Induced Electron Cloud in the LHC and Possible Remedies", these procoedings.

[5] H. Seiler, "Secondary electron emission in the scanning electron microscope", Phys. **54** (11) (1983).

[6] LHC Yellow book, CERN/AC/95-05 (LHC)

[7] V.Baglin et al, "Photoelectron yield and photon Reflectivity from candidate LHC vacuum chamber materials with implications to the vacuum chamber design"